PERGAMON

International Journal of Solids and Structures 40 (2003) 5707–5722

INTERNATIONAL JOURNAL OF SOLIDS and STRUCTURES

www.elsevier.com/locate/ijsolstr

Design of metallic textile core sandwich panels

F.W. Zok *, H.J. Rathbun, Z. Wei, A.G. Evans

College of Engineering III, Materials Department, University of California, Santa Barbara, CA 93106-5050, USA

Received 3 March 2003

Abstract

Metallic sandwich panels with textile cores have been analyzed subject to combined bending and shear and then designed for minimum weight. Basic results for the weight benefits relative to solid plates are presented, with emphasis on restricted optimizations that assure robustness (non-catastrophic failure) and acceptable thinness. Select numerical simulations are used to check the analytical results and to explore the role of strain hardening beyond failure initiation. Comparisons are made with competing concepts, especially honeycomb and truss core systems. It is demonstrated that all three systems have essentially equivalent performance. The influence on the design of a concentrated compressive stress that might crush the core has been explored and found to produce relatively small effect over the stress range of practical interest. "Angle ply" cores with members in the $\pm 45^\circ$ orientation are found to be near optimal for all combinations of bending, shear and compression.

Keywords: Sandwich panels; Lightweight structures; Textiles; Optimal design

1. Introduction

Concepts for metallic sandwich structures suitable for lightweight/multifunctional application have been presented in recent articles (Wicks and Hutchinson, 2001; Rathbun et al., submitted for publication; Deshpande and Fleck, 2001; Chiras et al., 2002; Mumm et al., 2002). Several truss core designs have been devised. Truss designs use the principle that, when incorporated into a panel and subjected to shear, the core members stretch/compress without bending. Tetrahedral, pyramidal and Kagome configurations satisfying this principle have been analyzed, fabricated and tested. Their basic attributes as lightweight structures have been ascertained by performing an optimization that finds the minimum weight needed to support specified loads without failure and then representing the results in non-dimensional, material independent coordinates (Wicks and Hutchinson, 2001). Comparisons with solid plates and honeycomb panels have been used to specify relative performance and cost benefits.

* Corresponding author. Tel.: +1-805-893-8699; fax: +1-805-893-8486.
E-mail address: zok@engineering.ucsb.edu (F.W. Zok).

0020-7683/$ - see front matter © 2003 Elsevier Ltd. All rights reserved.
doi:10.1016/S0020-7683(03)00375-5

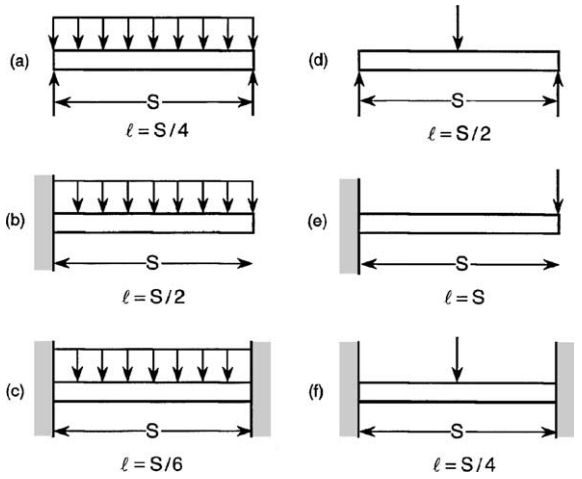

Fig. 1. Relationship between ℓ and loading span S for common test configurations, with (a)–(c) uniformly distributed pressure, and (d)–(f) concentrated loads.

For a panel subject to bending, supported over a span length, S, the load index combines the sustainable bending moment, M, and transverse shear, V (both per unit width) in the non-dimensional form (Wicks and Hutchinson, 2001):

$$\Pi = \frac{V}{\sqrt{EM}} \tag{1}$$

where E is the Young's modulus. The ratio of M and V defines a characteristic length scale, $\ell \equiv M/V$: which, since M and V vary with location, should be ascertained from the *maximum* values. Results for some common loading configurations are shown in Fig. 1. In all cases, ℓ is proportional to S, with a proportionality constant in the range 1/6–1. The panel weight per unit area, W, is conveniently expressed in the non-dimensional form: [1]

$$\Psi = \frac{W}{\rho \ell} \tag{2}$$

where ρ is the density of the material.

When comparing minimum weight results for different configurations, some practical constraints should be imposed. For example, lowest weights often coincide with panels having unacceptably large thickness, H_p, relative to span. Restricted optimizations are needed subject to, say, $H_p/\ell \leqslant 0.2$. Full consideration of all potential failure modes (notably, face yielding and wrinkling, as well as core member yielding and buckling) allows such comparisons (Fig. 2). The ensuing minimum weights and operative failure mechanisms depend on the yield strain for the material, ε_y, which must be specified when comparisons are made. A comparison for panels made with high yield strain alloys (representative of high strength Al) reveals that the tetrahedral truss core panel has essentially the same performance as the honeycomb core system (Fig. 2). The implication is that the benefits of the truss core do not reside in its performance, but rather, in lower manufacturing cost, especially in curved configurations, and when multifunctionality is exploited. The

[1] The weight index is consistent with the one in Wicks and Hutchinson (2001), but differs from that adopted by Evans (2001) and Mumm et al. (2002), notably $\Psi = W/\rho S$, by a factor (S/ℓ). This factor depends on loading configuration, as illustrated in Fig. 1.

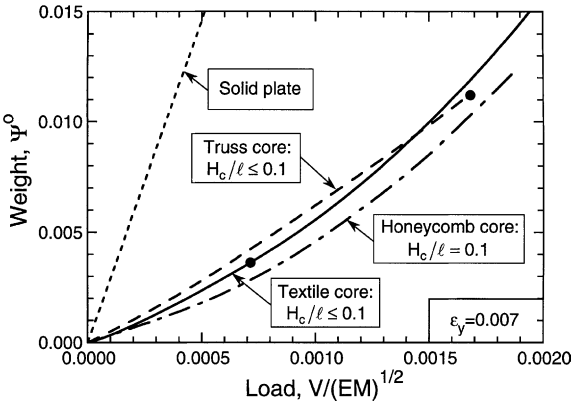

Fig. 2. Weight comparisons of optimized sandwich panels with one of three core types: textile, truss and honeycomb. Results for the truss core and honeycomb core panels taken from Wicks and Hutchinson (2001). The solid symbols on the curves for the textile core and the truss core panels indicate the points at which the core thickness reaches the prescribed limit: $H_c/\ell = 0.1$.

latter is exemplified by designing the panel to simultaneously bear load and provide cooling (Gu et al., 2001). Experimental assessments have demonstrated that manufacturing approaches rendering truss cores with wrought (rather than cast) properties are preferred (Rathbun et al., submitted for publication; Sypeck and Wadley, 2002), because of superior robustness, as well as lower costs.

One approach for the design and manufacturing of wrought cores uses textile technology (Mumm et al., 2002). Woven metal textiles are stacked and transient liquid phase (TLP) bonded at the nodes, followed by TLP bonding to face sheets. The approach has the potential for lower cost than both truss cores and honeycombs because of the lower material costs as well as the relative simplicity of the fabrication. The basic concept has been demonstrated (Mumm et al., 2002): but the assessment was confined to cores with relative density ($\bar{\rho}_c \approx 0.2$) much larger than those pertinent to minimum weight designs. This article elaborates on the concept, with the objective of finding optimal configurations and comparing with truss and honeycomb designs.

One of the key findings of the initial study (Mumm et al., 2002) was the criticality of the textile core orientation. Namely, in the 0°/90° orientation, the textile core members experience bending when a shear is imposed, resulting in low strength and stiffness. Conversely, in the ±45° orientation, the members experience either tension or compression (no bending) resulting in a strong/stiff core. This orientation and other $\pm\gamma^\circ$ configurations are emphasized in this study. The ensuing analyses use simplified expressions for the stresses, neglecting details at textile crossovers and attachments to the faces. To be conservative, the "failures" coincide with the onset of either yield or buckling. In practice, for certain failure modes, strain hardening can lead to limit loads significantly in excess of the onset conditions. The associated enhancements in load capacity are explored by means of selected numerical simulations.

The practical implementation of sandwich panels is often limited by failure caused by concentrated compressive stresses. In such cases, the cores can crush locally, accompanied by plastic hinging of the outer face (Ashby et al., 2000). The incidence of this failure mode is most strongly affected by the compressive strength of the core. This mode is analyzed and used as a new constraint on the minimum weight design.

A logical evolution of ideas governing the designs is facilitated by using the following organization.

(i) The textile geometry is described.
(ii) The failure modes are analyzed.
(iii) To ascertain minimum weights, an optimization is performed for panels subject to combinations of bending and shear.

(iv) Restricted optimizations are performed that ensure robustness and also impose limits on panel thickness.
(v) A comparison is made with solid panels at equivalent weight.
(vi) Numerical simulations are performed to assess the analytical results and to explore effects of strain hardening.
(vii) Textile core panels are compared with competing concepts.
(viii) The effects on the minimum weights of concentrated compressive loads are examined.
(ix) The influence of the textile "ply angle" on the performance is analyzed.

Unless otherwise stated, all of the results are presented for a material with yield strain, $\varepsilon_y = 0.001$, representative of steels, as well as Ni and Cu alloys. A few results are presented for $\varepsilon_y = 0.004$ and 0.007, pertinent to some high strength Al and Ti alloys.

2. Geometry

The textile core panel (Fig. 3) consists of two face sheets, thickness t_f, and a core, thickness H_c. The core and the face sheets are made from the same material, with Young's modulus E, yield strength σ_y, and density ρ. The wires comprising the core have radius R and a separation length L. The spacing between the textile layers, measured normal to the plane of Fig. 3, is $2\alpha R$ where $\alpha \approx 2$. For most of the subsequent analysis, the $\pm 45°$ orientation is explored. It will be shown that, absent transverse compression, this configuration is optimal. When a transverse compression is superposed, the preferred configuration changes to a $\pm\gamma$ "angle ply" with $\gamma < 45°$ (Section 10).

The wires are considered well bonded both at the crossovers and at the face sheets. The attachments to the face sheets are uncorrelated between adjacent layers. [2] The absence of a periodic arrangement across the panel precludes face sheet buckling, thereby excluding one of the failure mechanisms found in truss core panels (Wicks and Hutchinson, 2001). But it introduces an alternate potential failure mode, notably face wrinkling (Ashby et al., 2000).

Provided that $L/R \gg 1$, the relative core density $\overline{\rho}_c$ can be approximated by:

$$\overline{\rho}_c \approx \frac{\pi R}{\alpha L} \tag{3}$$

Furthermore, if $H_c/t_f \gg 1$, the sandwich panel thickness, H_p, can be approximated by $H_p = 2t_f + H_c \approx H_c$. The non-dimensional weight index then becomes:

$$\Psi = \frac{2t_f}{\ell} + \frac{\overline{\rho}_c H_c}{\ell} = \frac{2t_f}{\ell} + \frac{\pi R H_c}{\alpha L \ell} \tag{4}$$

Eq. (4) is the objective function that we seek to minimize.

3. Failure modes under bending and shear

3.1. Core failure

The core experiences failure as a consequence of the shear force, V. The core members are regarded as slender columns that support only axial load and no bending moment. Then, the average axial stress in the core members, σ_z, is related to V by:

[2] The degree of correlation in the attachment points can be tailored in the manufacturing operation. Highly periodic arrangements have been obtained (Mumm et al., 2002), although random ones can be made also (Wadley, 2003).

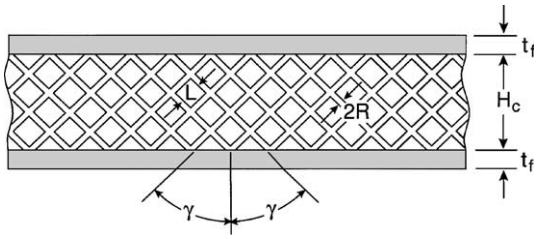

Fig. 3. Schematic of the textile core sandwich panel.

$$\sigma_z = \frac{2\alpha L V}{\pi R H_c} \tag{5}$$

Equating σ_z to the yield strength of the members, σ_y, gives the transverse shear load upon core yielding (Mumm et al., 2002):

$$V_y = \frac{\pi R H_c \sigma_y}{2\alpha L} \tag{6}$$

Elastic buckling of the core members is strongly affected by the rotational stiffness of the crossovers. For conservatism, we assume that the crossovers are pin-jointed ($k = 1$) and that L is the buckling half-wavelength. In practice, the rotational stiffness of the nodes could enhance the strength by a factor 2. Equating the axial member stress (Eq. (5)) to the Euler buckling stress (Timoshenko and Gere, 1961), the critical shear load becomes:

$$V_B = \frac{k\pi^3 E R^3 H_c}{8\alpha L^3} \tag{7}$$

3.2. Failure in the faces

The face failure modes are dictated by the bending moment, M. Face yielding occurs when the normal stress reaches the yield strength, which occurs at bending moment (Ashby et al., 2000)

$$M_y = t_f H_c \sigma_y \tag{8}$$

Provided the spacing between attachment points is smaller than the face sheet thickness, face wrinkling occurs when (Ashby et al., 2000)

$$M_w = t_f H_c \varsigma E \left(\frac{\overline{\rho}_c}{2}\right)^{2/3} \tag{9}$$

where $\varsigma \approx 0.58$. This result may be non-conservative when the attachment spacing exceeds the face sheet thickness. Nevertheless, the subsequent results show that this failure mode is operative in the optimized structures only at exceedingly low loads, well below those of practical interest. Consequently, refinements to the critical bending moment are deemed unnecessary for the current design optimization.

4. Design optimization

An optimization has been performed to determine the minimum weight, subject to the requirement that the panel support a prescribed combination of M and V without failure. All length scales are normalized by

ℓ (Wicks and Hutchinson, 2001). The four parameters characterizing the panel geometry are: $x_1 \equiv t_f/\ell$, $x_2 \equiv R/\ell$, $x_3 \equiv L/\ell$, and $x_4 \equiv H_c/\ell$. Accordingly, the objective function (Eq. (4)) is re-written as:

$$\Psi = 2x_1 + \frac{\pi x_2 x_4}{\alpha x_3} \tag{10}$$

4.1. The constraints

The constraints are dictated by the four failure modes (Eqs. (6)–(9)). Upon normalizing, the parameters x_3 and x_2 appear only as a ratio, $\eta \equiv x_3/x_2 = L/R$, enabling the constraints to be expressed as:

$$\left(\frac{V^2}{EM}\right)\left(\frac{1}{\varepsilon_y x_1 x_4}\right) \leqslant 1 \text{ Face yielding} \tag{11a}$$

$$\left(\frac{V^2}{EM}\right)\left(\frac{1}{\varsigma x_1 x_4}\right)\left(\frac{2\alpha\eta}{\pi}\right)^{2/3} \leqslant 1 \text{ Face wrinkling} \tag{11b}$$

$$\left(\frac{V^2}{EM}\right)\left(\frac{2\alpha\eta}{\pi x_4 \varepsilon_y}\right) \leqslant 1 \text{ Core yielding} \tag{11c}$$

$$\left(\frac{V^2}{EM}\right)\left(\frac{8\alpha\eta^3}{\pi^3 k x_4}\right) \leqslant 1 \text{ Core buckling} \tag{11d}$$

4.2. Confluence of failure mechanisms

The design point at which *face yielding and wrinkling* occur simultaneously is obtained by equating the left sides of Eqs. (11a) and (11b). The result can be expressed in terms of either a critical aspect ratio,

$$\eta^* \equiv \left(\frac{L}{R}\right)^* = \frac{\pi}{2\alpha}\left(\frac{\varsigma}{\varepsilon_y}\right)^{3/2} \tag{12a}$$

or a critical core density (via Eq. (3)):

$$\overline{\rho}_c^* = 2\left(\frac{\varepsilon_y}{\varsigma}\right)^{3/2} \tag{12b}$$

For typical yield strains ($\varepsilon_y \approx 0.001$), face wrinkling occurs for aspect ratios greater than $(L/R)^* = 10^4$ and core densities less than $\overline{\rho}_c^* = 10^{-4}$, well outside the practical range. Consequently, the optima are attained at the confluence of the three remaining potential failure modes.

Simultaneous *face yielding and core buckling* is characterized by setting the constraints in Eqs. (11a) and (11d) equal to unity and combining the result with the objective function (Eq. (10)). This yields the non-dimensional weight:

$$\Psi = \frac{k\pi^3}{4\alpha\eta^3\varepsilon_y} + \frac{8V^2\eta^2}{EMk\pi^2} \tag{13}$$

The minimum weight and the associated geometric parameters are obtained by setting $\partial\Psi/\partial\eta = 0$, giving

$$\Psi^o = \frac{5}{3}\left(\frac{V}{\sqrt{EM}}\right)^{6/5}\left(\frac{6}{\alpha\varepsilon_y}\right)^{2/5}\left(\frac{2}{k}\right)^{1/5} \tag{14a}$$

$$\eta^{\mathrm{o}} = \pi\left(\frac{V}{\sqrt{EM}}\right)^{-2/5}\left(\frac{3k^2}{64\alpha\varepsilon_y}\right)^{1/5} \tag{14b}$$

$$x_1^{\mathrm{o}} = \left(\frac{V}{\sqrt{EM}}\right)^{6/5}\left(\frac{8}{27k\alpha^2\varepsilon_y^2}\right)^{1/5} \tag{14c}$$

$$x_4^{\mathrm{o}} = \left(\frac{V}{\sqrt{EM}}\right)^{4/5}\left(\frac{27\alpha^2 k}{8\varepsilon_y^3}\right)^{1/5} \tag{14d}$$

Upon comparing Eqs. (11c) and (11d), it becomes apparent that, once L/R diminishes below a transition value, η_{tr}, core failure occurs by yielding rather than buckling. The transition happens when:

$$\eta_{\mathrm{tr}} = \frac{\pi}{2}\left(\frac{k}{\varepsilon_y}\right)^{1/2} \tag{15}$$

Once Eq. (15) is satisfied, thereafter the optimum occurs at the confluence of *face and core yielding*. The optimum is coincident with the lowest core density that consistently permits failure by yielding (that is, when $\eta = \eta_{\mathrm{tr}}$), giving:

$$\Psi^{\mathrm{o}} = \frac{2}{\alpha\lambda}\left(\frac{\varepsilon_y}{k}\right)^{1/2} + \left(\frac{V^2}{EM}\right)\left(\frac{2}{\varepsilon_y}\right) \tag{16}$$

For this design, the three failure modes occur concurrently. The optimal core thickness in this domain is:

$$x_4^{\mathrm{o}} = \left(\frac{\alpha\sqrt{k}}{\varepsilon_y^{3/2}}\right)\left(\frac{V^2}{EM}\right) \tag{17}$$

The critical core thickness at which core yielding is activated in the optimized panel is obtained from a comparison of Eqs. (14d) and (17). This occurs at $x_4^* = H_{\mathrm{c}}/\ell = 3/2$. The implication is that extremely thick panels are required, well beyond the range representative of thin plates. Consequently, this domain is neglected in the subsequent restricted optimizations and weight comparisons.

4.3. Optimal designs

The results of the optimization are plotted in Fig. 4, for $\alpha = 2$, $k = 1$, and yield strains $\varepsilon_y = 0.001$, 0.004 and 0.007. The active failure modes are core buckling and face yielding over essentially the entire load range. [3] Also shown for comparison is the weight of a solid plate with a strength equivalent to that of the sandwich panel, given by:

$$\Psi_{\mathrm{s}} = \left(\frac{6E}{\sigma_y}\right)^{1/2}\frac{V}{\sqrt{EM}} \tag{18}$$

The weight benefits of the sandwich panels over the solid plate are evident.

[3] The exception is that face wrinkling becomes active at extremely low loads, typically $V/\sqrt{EM} < 10^{-7}$.

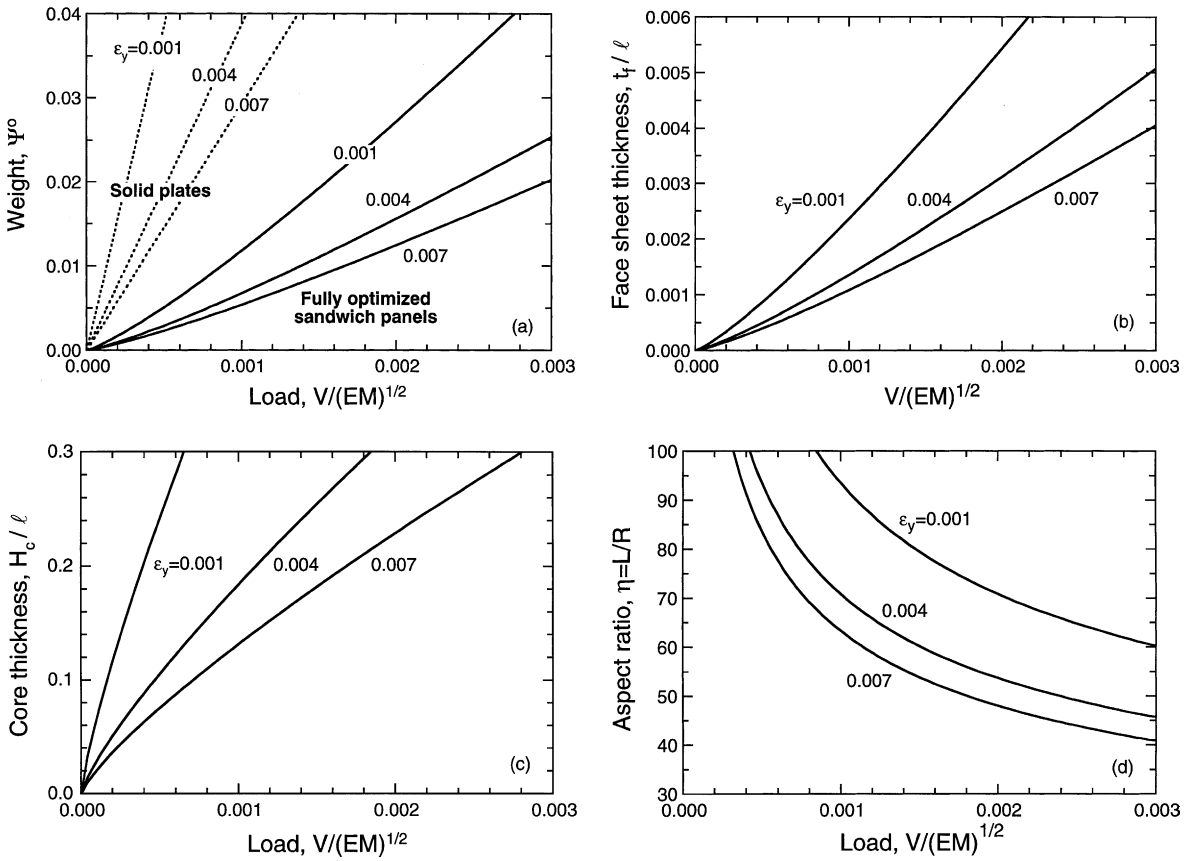

Fig. 4. Sandwich panels optimized for shear and bending, showing effects of the yield strain. Face yielding and core buckling are active over the load range shown. Results are based on parameter values $\alpha = 2$ and $k = 1$. Although not shown here, the effects of k are small; since the weight scales as $k^{-1/5}$, using the upper limit of $k = 2$ would produce a weight reduction of 13%.

5. Restricted optimizations

5.1. Robustness

The preceding optimizations require that the panel support a prescribed combination on M and V up to initial failure. For robust performance beyond initiation, modes that allow significant plastic deformation without localization are preferred. Elastic core buckling is the least desirable. Core yielding is also undesirable since it is superceded by unstable plastic buckling at quite small plastic strains. Face yielding is the most desirable since large deformations can occur without instability. Accordingly, to design lightweight panels that are both strong and robust, a series of restricted optimizations can be performed for parameters that lead to face yielding. This objective is accomplished by fixing η below the buckling threshold (Eq. (14b)) and restricting the loads to avert core yielding.

Optimal designs are obtained by first combining the constraint in Eq. (11a) with the objective function in Eq. (10). The result is

$$\Psi = \left(\frac{2}{x_4 \varepsilon_y}\right)\left(\frac{V^2}{EM}\right) + \frac{\pi x_4}{\alpha \eta} \tag{19}$$

The optimal values, obtained by setting $(\partial \Psi/\partial x_4)_\eta = 0$, are

$$\Psi^{\mathrm{o}} = \frac{2V}{\sqrt{EM}}\left(\frac{2\pi}{\alpha\eta\varepsilon_y}\right)^{1/2} \tag{20a}$$

$$x_1^{\mathrm{o}} = \frac{V}{\sqrt{EM}}\left(\frac{\pi}{2\alpha\eta\varepsilon_y}\right)^{1/2} \tag{20b}$$

$$x_4^{\mathrm{o}} = \frac{V}{\sqrt{EM}}\left(\frac{2\alpha\eta}{\pi\varepsilon_y}\right)^{1/2} \tag{20c}$$

$$\frac{x_4^{\mathrm{o}}}{x_1^{\mathrm{o}}} \equiv \frac{H_{\mathrm{c}}}{t_{\mathrm{f}}} = \frac{2\alpha\eta}{\pi} \equiv \frac{4L}{\pi R} \tag{20d}$$

The results are compared with those of the fully optimized panels in Fig. 5(a). Note that the strength benefit diminishes with decreasing η because the panels are non-optimal. However, such panels should be more robust. Note that the design characterized by Eq. (20d) is independent of both the load index, $V/\sqrt{EM}$ and the yield strain, ε_y. Such simple rules do not emerge for the fully optimized panel.

5.2. Core thickness

The restriction on core thickness is imposed for the domain in which face yielding and core buckling occur concurrently. The constraints in Eqs. (11a) and (11c) are combined with Eq. (10), but now x_4 is taken to be constant, at a prescribed $x_4^{\max}$. The resulting panel weight is

$$\Psi^{\mathrm{o}} = \left(\frac{V}{\sqrt{EM}}\right)^2 \frac{2}{\varepsilon_y x_4^{\max}} + \left(\frac{8}{k}\right)^{1/3}\left(\frac{x_4^{\max}}{\alpha}\frac{V}{\sqrt{EM}}\right)^{2/3} \tag{21}$$

The results for $x_4^{\max} = 0.1$, 0.2 and 0.3 are plotted on Fig. 5(a). At small loads, the core thickness for the optimized panel falls below the prescribed limit, negating the restriction. At large loads, the limiting core

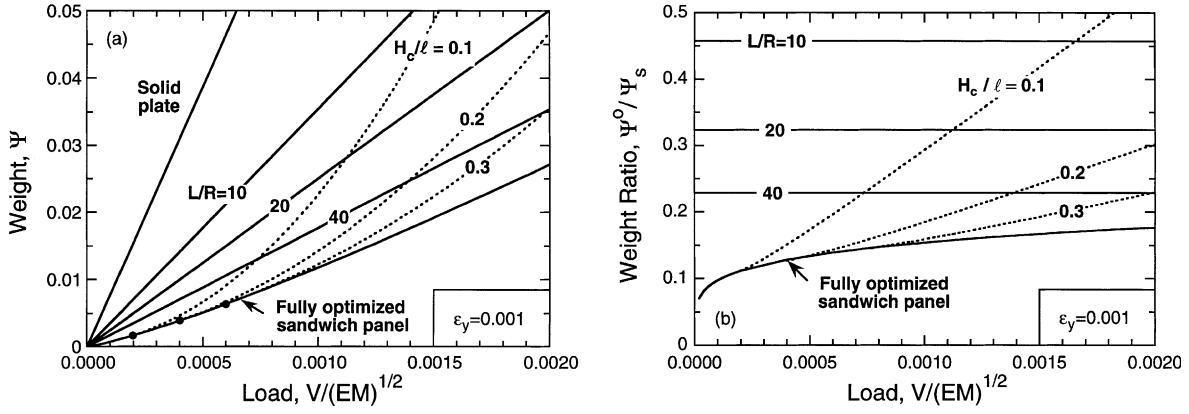

Fig. 5. (a) Comparisons of fully optimized sandwich panels with those restricted to having either a fixed L/R or a maximum H_c/ℓ. Solid symbols show the points at which the core thickness in the fully optimized panel reaches one of the three prescribed limits: $H_c/\ell = 0.1$, 0.2 or 0.3. (b) A re-interpretation of the results in (a), showing weight reduction relative to a solid plate.

thickness dominates the design. In the latter, while the weight benefit of the sandwich panel diminishes, the performance remains superior to that of the solid plate.

6. Weight comparisons with solid plates

To quantify the weight benefits, the preceding optimizations have been re-expressed in terms of the ratio of the weight of the sandwich panel to that of the solid plate. The pertinent ratios are as follows.

(i) For the fully optimized panel:

$$\frac{\Psi^{\mathrm{o}}}{\Psi_{\mathrm{s}}} = \frac{5}{3}\left(\frac{2}{\alpha^2 k}\frac{V}{\sqrt{EM}}\right)^{1/5}\left(\frac{\varepsilon_y}{6}\right)^{1/10} \tag{22a}$$

(ii) For robust panels designed to fail by face yielding:

$$\frac{\Psi^{\mathrm{o}}}{\Psi_{\mathrm{s}}} = \left(\frac{4\pi}{3\alpha\eta}\right)^{1/2} \equiv \sqrt{\frac{2R}{L}} = 1.1\sqrt{\bar{\rho}_{\mathrm{c}}} \tag{22b}$$

(iii) For panels that must be thinner than a prescribed thickness:

$$\frac{\Psi^{\mathrm{o}}}{\Psi_{\mathrm{s}}} = \frac{2V}{\sqrt{EM}}\left(\frac{1}{6\varepsilon_y}\right)^{1/2}\frac{1}{x_4^{\max}} + \left(\frac{x_4^{\max}}{\alpha}\right)^{2/3}\left(\frac{8}{k}\right)^{1/3}\left(\frac{\varepsilon_y}{6}\right)^{1/2}\left(\frac{V}{\sqrt{EM}}\right)^{1/6} \tag{22c}$$

The results are plotted in Fig. 5(b). Note that, for the panel designed to fail by face yielding, the weight is independent of the load index and yield strain and given simply by: $\Psi^{\mathrm{o}}/\Psi_{\mathrm{s}} = 1.1\sqrt{\bar{\rho}_{\mathrm{c}}}$. Recall that the corresponding design rule is: $H_{\mathrm{c}}/t_{\mathrm{f}} = 2/\bar{\rho}_{\mathrm{c}}$.

7. Numerical results

Select numerical simulations have been performed with two objectives: (a) to verify the results presented on Fig. 5, and (b) to examine the robustness that can be realized with a strain hardening material subsequent to failure initiation. For this purpose, a constitutive law for the textile core has been devised and implemented in the ABAQUS finite element code. It is based on the law derived for foam cores, modified to fit the deformation characteristics of the textile system (Ashby et al., 2000; Wei et al., 2003). The constitutive law is elliptic (no corners), containing terms associated with yielding subject to shear and pressure. The calibration of the unknown coefficients involves tests and analysis conducted for combinations of shear and pressure that probe the ellipticity of the surface. Strain hardening can be incorporated by using as input the stress/strain curve measured in uniaxial compression.

To be conservative, the core response has been taken to be elastic/perfectly plastic, with compressive yield stress $\sigma_y^{\mathrm{c}} \approx \sigma_y \bar{\rho}_{\mathrm{c}}/2$ and shear yield stress $\tau_y^{\mathrm{c}} = \sigma_y^{\mathrm{c}}$. To assess performance in the face yielding domain, the core member aspect ratio has been varied over the range $10 \leqslant L/R \leqslant 40$ and the relative core thickness taken to be $H_{\mathrm{c}}/t_{\mathrm{f}} = 4L/\pi R$ (Eq. (20d)). The plate dimensions were varied to produce H_{c}/ℓ in the range 0.1–0.4. The elastic/plastic response of the face sheets was selected to represent annealed stainless steels: Young's modulus $E = 200$ GPa, yield strength $\sigma_y = 200$ MPa and linear hardening after yield with a tangent modulus $E_T = E/100 = 2$ GPa. The simulated plates were built-in, and loaded either by a concentrated center load (Fig. 1(f)) or by a uniformly distributed pressure (Fig. 1(c)).

Results for strength, defined by the onset of face yielding, are plotted in Fig. 6, and compared with the analytical solutions (Eqs. (20)). The simulations yield a slightly higher strength at given weight, by about

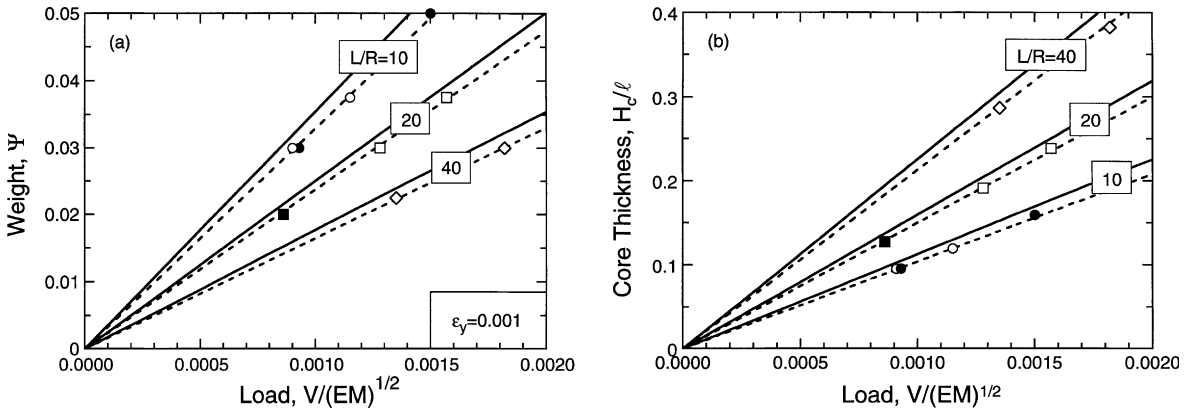

Fig. 6. Comparisons of numerical results (symbols) with analytical model (solid lines), for restricted optimizations with fixed L/R: (a) panel weight, and (b) core thickness. Solid symbols are for a concentrated center load (Fig. 1 (f)) and open symbols for a uniformly distributed pressure (Fig. 1 (c)).

5–10%. This is consistent with the conservative assumptions in the analytical model, notably: (i) that $H_p \approx H_c$, (ii) that the bending is carried solely by the face sheets and (iii) that the shear is carried solely by the core. Each simplification leads to a slight underestimate in strength, although the combined effect remains comparatively small. Interestingly, the analytical model provides accurate estimates even for the thickest cores used in the simulations, $H_c/\ell \approx 0.4$.

The normalized load–displacement responses, $\Sigma(\Delta)$, are plotted in Fig. 7, illustrating the effect of core member aspect ratio, L/R, at fixed panel weight ($\Psi = 0.03$). For these normalizations, yielding initiates in the solid plate at $\Sigma = 1$, $\Delta = 1$. Note that the sandwich panels exhibit significant elevations in strength over the solid plate, with the advantages increasing linearly with L/R: attaining $\Sigma > 10$ for the highest L/R. Equally significant is the rise in the load–displacement response beyond initial yield. For instance, for $L/R = 40$, the load-bearing capacity is nearly doubled, $\Sigma/\Sigma_y \approx 2$, after a displacement $\Delta/\Delta_y \approx 5$ (where Δ_y

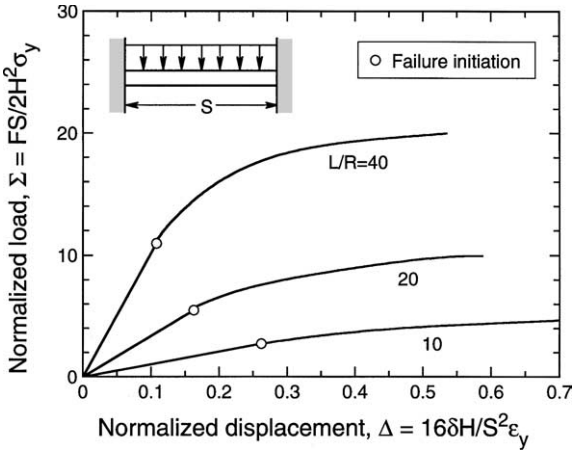

Fig. 7. Numerical simulations of load–displacement response of sandwich panels subjected to a uniformly distributed pressure, each of weight $\Psi = 0.03$, but with varying L/R. Here H is the thickness of the equivalent solid plate and P is the total load. For reference, the yield load of the equivalent solid plate is $\Sigma = 1$.

and Σ_y are the displacement and load at yield). Such robust behavior would not be obtained in panels designed to fail by buckling.

8. Comparisons with competing concepts

Comparisons have been made with two competing sandwich concepts: one based on a truss core in a tetrahedral configuration and the other a honeycomb core (Wicks and Hutchinson, 2001). Weight comparisons have been presented in Fig. 2 for panels with $\varepsilon_y = 0.007$. The results for the truss core panels are based on a full optimization, analogous to that presented above in Section 4. Over the entire load range used in the figure, the thickness of the optimized truss core panel satisfies a thin plate requirement, $H_c/\ell \leqslant 0.1$. The optimized honeycomb core panel is exceedingly thick over the same load range. Accordingly, for a meaningful comparison, the results have been restricted to a core thickness, $H_c/\ell = 0.1$. The optimized textile core panels are intermediate in the sense that the cores satisfy the thin plate requirement to the left of the solid symbol, but to the right are restricted by $H_c/\ell = 0.1$.

The comparisons indicate that there is essentially no difference between the three core topologies. Consequently, as surmised above, the benefits of the textile system reside in lower manufacturing cost, especially in non-planar configurations, and when multifunctionality is utilized. Differences in robustness, following failure initiation, have yet to be explored.

9. Panels with superposed compressive loads

The preceding optimizations have been extended to include the influence of a concentrated compression, σ, at the loading points, having magnitude relative to the shear stress characterized by a non-dimensional parameter,

$$\beta \equiv \frac{\sigma H_c}{V} \tag{23}$$

For cases of practical interest, the compression is bounded approximately by $0 \leqslant \beta \leqslant 2$ (Appendix A). The axial member stress due to the combined action of the compression and the shear is:

$$\sigma_z = \frac{2\alpha L V(1+\beta)}{\pi R H_c} \tag{24}$$

The modified constraints for core failure are obtained by setting σ_z equal to the critical values for yielding and buckling. The results are:

$$\left(\frac{V^2}{EM}\right)\left(\frac{2\alpha\eta(1+\beta)}{\pi x_4 \varepsilon_y}\right) \leqslant 1 \text{ Core yielding} \tag{25a}$$

$$\left(\frac{V^2}{EM}\right)\left(\frac{8\alpha\eta^3(1+\beta)}{k\pi^3 x_4}\right) \leqslant 1 \text{ Core buckling} \tag{25b}$$

The constraints for face failure remain unchanged (Eqs. (11a) and (11b)).

The optimal values of the weight and the associated geometric parameters are obtained through the optimization procedure described in Section 4. For the domain wherein face yielding and core buckling are active, the optimal values are:

$$\Psi^{o} = \frac{5}{3}\left(\frac{V}{\sqrt{EM}}\right)^{6/5}\left(\frac{6}{\alpha\varepsilon_y}\right)^{2/5}\left(\frac{2(1+\beta)}{k}\right)^{1/5} \tag{26a}$$

$$\eta^{o} = \pi\left(\frac{V}{\sqrt{EM}}\right)^{-2/5}\left(\frac{3k^2}{64\alpha\varepsilon_y(1+\beta)^2}\right)^{1/5} \tag{26b}$$

$$x_1^{o} = \left(\frac{V}{\sqrt{EM}}\right)^{6/5}\left(\frac{8(1+\beta)}{27k\alpha^2\varepsilon_y^2}\right)^{1/5} \tag{26c}$$

$$x_4^{o} = \left(\frac{V}{\sqrt{EM}}\right)^{4/5}\left(\frac{27\alpha^2 k}{8\varepsilon_y^3(1+\beta)}\right)^{1/5} \tag{26d}$$

At high loads, core yielding is active also. But, as for the case with only shear and bending, this mode is activated only for very thick cores: specifically $x_4^* = H_c/\ell = 3/(2(1+\beta))$. For $\beta = 2$, $x_4^* = 0.5$, beyond the limit of thin plates.

The increase in weight due to the added compression is small: varying as $(1+\beta)^{1/5}$ in the domain of interest, where face yielding and core buckling are active (Fig. 8(a)). For instance, in an extreme case, wherein the magnitude of the compression equals the shear ($\beta = 1$), the panel is about 15% heavier. The effects of compression on the geometric parameters are similarly small, as evidenced by the weak power law scalings with $(1+\beta)$ in Eqs. 26(b)–(d).

10. Optimal weave angle

In this section, the optimal weave angle γ^{o} for combined bending, shear and compressive loads is derived. The core density and panel weight for an arbitrary weave angle γ are given approximately by:

$$\overline{\rho}_c = \frac{\pi}{2\alpha\eta\sin\gamma\cos\gamma} \tag{27a}$$

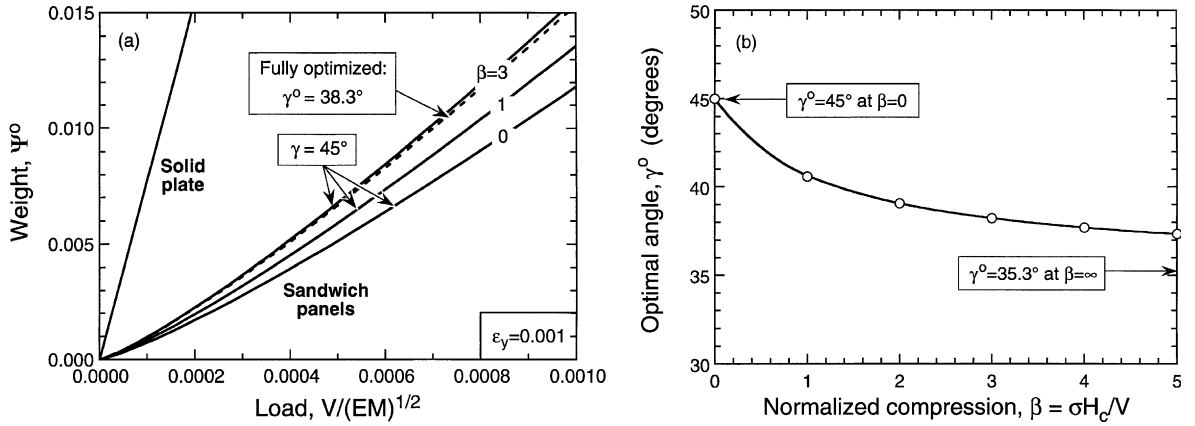

Fig. 8. Sandwich panels optimized for compression, shear and bending. Effects of compression, β, on (a) weight of optimized panel and (b) optimal weave angle γ^{o}.

$$\Psi = 2x_1 + \frac{\pi x_4}{2\alpha\eta \sin\gamma \cos\gamma} \tag{27b}$$

Noting that the axial member stress is:

$$\sigma_z = \frac{2\alpha LV(1+\beta\tan\gamma)}{\pi R H_c} \tag{28}$$

the constraints for core failure become:

$$\left(\frac{V^2}{EM}\right)\left(\frac{2\alpha\eta(1+\beta\tan\gamma)}{\pi x_4 \varepsilon_y}\right) \leqslant 1 \text{ Core yielding} \tag{29a}$$

$$\left(\frac{V^2}{EM}\right)\left(\frac{8\alpha\eta^3(1+\beta\tan\gamma)}{k\pi^3 x_4}\right) \leqslant 1 \text{ Core buckling} \tag{29b}$$

The constraints for face failure remain unchanged (Eqs. (11a) and (11b)). The optimal values of η and γ are obtained by first equating the left sides of Eqs. (11a) and (29b), then combining with the modified objective function, Eq. (27b), and, finally, setting $(\partial\Psi/\partial\gamma)_\eta = 0$ and $(\partial\Psi/\partial\eta)_\gamma = 0$. The results of this procedure are as follows.

The optimal weave angle is given by the implicit function:

$$\frac{\cos^2\gamma^o}{\beta}(1+\beta\tan\gamma^o)(\cot\gamma^o - \tan\gamma^o) = \frac{1}{3} \tag{30a}$$

The solution (Fig. 8(b)) indicates that, in the limit $\beta = 0$ (no compression), the optimal angle is $\gamma^o = 45°$, as already noted. In another limit, $\beta \to \infty$, the optimum is $\gamma^o = 35.3°$. The corresponding panel weight and optimal aspect ratio for all β are:

$$\Psi^o = \frac{5}{3}\left(\frac{V}{\sqrt{EM}}\right)^{6/5}\left(\frac{3}{\alpha\varepsilon_y}\right)^{2/5}\left(\frac{1}{k}\right)^{1/5}\frac{(1+\beta\tan\gamma^o)^{1/5}}{(\sin\gamma^o\cos\gamma^o)^{3/5}} \tag{30b}$$

$$\eta^o = \frac{\pi}{2}\left(\frac{V}{\sqrt{EM}}\right)^{-2/5}\left(\frac{3k^2}{\alpha\varepsilon_y}\right)^{1/5}\left(\frac{\sin\gamma^o\cos\gamma^o}{(1+\beta\tan\gamma^o)^2}\right)^{1/5} \tag{30c}$$

Representative results for the minimum weight (Fig. 8(a)) indicate that the effects of weave angle are exceedingly small. The maximum benefit arises for large β. But even in the limit $\beta \to \infty$, the optimized panel is only 3.3% lighter. Accordingly, cores with $\gamma = 45°$ are near optimal for all load combinations.

11. Concluding remarks

Textile core sandwich panels can be designed to support bending and shear loads with weights as much as an order of magnitude lower than that of an equivalent solid plate. When designed to a failure initiation criterion, the textile core panels are comparable to those utilizing other lightweight cores, including honeycombs and trusses. Experiments are in progress to validate the failure models, as well as the comparisons of the core topologies on the basis of robustness, for combined compressive, bending and shear loads. New metrics that combine performance and manufacturing cost into a single structural index are being devised as a means for allowing explicit selection of the preferred core.

Acknowledgements

This work was supported by the ONR MURI program on Blast Resistant Structures through a subcontract from Harvard University to the University of California at Santa Barbara (Contract No. 123163-03).

Appendix A

When bending moments are induced through concentrated transverse loads, failure can occur by indentation at the loading points. This mode involves yielding of the core and formation of plastic hinges within the face sheet adjacent to the indenter. Analysis yields a critical indentation pressure, P_I, given by (Ashby et al., 2000):

$$P_I = \sigma_y^c + \frac{2t_f}{w}\sqrt{\sigma_y^c \sigma_y^f} \tag{A.1}$$

where w is the width of the indenter used for applying load; σ_y^f is the yield strength of the face sheets; and σ_y^c is the compressive yield strength of the core, given approximately by (Mumm et al., 2002):

$$\sigma_y^c \approx \frac{\sigma_y \overline{\rho}_c}{2} \tag{A.2}$$

Combining Eqs. (A.1) and (A.2), and assuming that the face sheets and the core are made of the same material, with yield strength σ_y, the indentation pressure becomes:

$$P_I = \sigma_y^c \left(1 + \frac{2t_f}{w}\sqrt{\frac{2}{\overline{\rho}_c}}\right) \tag{A.3}$$

For loading configurations of practical interest (Figs. 1(d)–(f)), w is selected to be at least as large as the panel thickness: $w = \kappa H_c$ where $\kappa \geqslant 1$. Moreover, for the sandwich panels under consideration here, typically $H_c/t_f \geqslant 10$, leading to $w/t_f \geqslant 10\kappa$. In this domain, the indentation pressure in Eq. (A.3) can be approximated by $P_I \approx \sigma_y^c$. That is, indentation is resisted predominantly by the core, with minimal contribution from the face sheet. This result is conservative for finite w/t_f and exact for a uniformly distributed pressure (Figs. 1(a)–(c)).

On this basis, the normalized compressive stress β can be obtained by taking the transverse compression within the core to be equal to the indenter pressure and combining with the maximum shear force V in the configuration of interest. For three point bending (either simply supported or built-in), $V = F/2$, with F being the applied force, and $P = F/w$. This yields $\beta = 2/\kappa$. Similarly, for a cantilever beam, $\beta = 1/\kappa$. Thus, for $\kappa \geqslant 1$, the limits on compression for both test configurations become $0 \leqslant \beta \leqslant 2$.

The results in Fig. 8(a) extend out to $\beta = 3$ and demonstrate the rather weak sensitivity of the design to β. An even weaker dependence is obtained on the weave angle, γ.

References

Ashby, M.F., Evans, A.G., Fleck, N.A., Gibson, L.J., Hutchinson, J.W., Wadley, H.N.G., 2000. Metal Foams: A Design Guide. Butterworth Heinemann, Boston.

Chiras, S., Mumm, D.R., Evans, A.G., Wicks, N., Hutchinson, J.W., Dharmasena, K., Wadley, H.N.G., Fichter, S., 2002. The structural performance of near-optimized truss core panels. International Journal of Solids and Structures 39, 4093–4115.

Deshpande, V.S., Fleck, N.A., 2001. Collapse of truss core sandwich beams in 3-point bending. International Journal of Solids and Structures 38, 6275–6305.

Evans, A.G., 2001. Lightweight materials and structures. MRS Bulletin 26, 790.

Gu, S., Lu, T.J., Evans, A.G., 2001. On the design of two-dimensional cellular metals for combined heat dissipation and structural load capacity. International Journal of Heat and Mass Transfer 44, 2163–2175.

Mumm, D.R., Chiras, S.J., Evans, A.G., Hutchinson, J.W., Sypeck, D.J., Wadley, H.N.G., 2002. On the performance of light weight metallic panels fabricated using textile technology. International Journal of Solids and Structures.

Rathbun, H.J., Wei, Z., He, M.Y., Zok, F.W., Evans, A.G., Sypeck, D.J., Wadley, H.N.G., submitted for publication. Measurements and simulations of the performance of metallic sandwich structures with a near optimal tetrahedral truss core. Journal of Applied Mechanics.

Sypeck, D.J., Wadley, H.N.G., 2002. Cellular metal truss core sandwich structures. Advanced Engineering Materials 4, 759–764.

Timoshenko, S.P., Gere, J.M., 1961. Theory of Elastic Stability. McGraw-Hill, New York.

Wadley, H.N.G., 2003. Private communication.

Wei, Z., He, M.Y., Evans, A.G., 2003. Unpublished research, University of California, Santa Barbara.

Wicks, N., Hutchinson, J.W., 2001. Optimal truss plates. International Journal of Solids and Structures 38, 5183–6165.